How the phosphorus chains impact on the vibrational properties of diphosphides ZnP$_2$ and CdP$_2$ at low temperatures

K.V. Shportko
V. Lashkaryov Institute of Semiconductor Physics, National Academy of Sciences of Ukraine
45, prospect Nauky, 03680 Kyiv Ukraine, e-mail: konstantin@shportko.com

Abstract. The temperature dependence of the vibrational modes in the diphosphides ZnP$_2$ and CdP$_2$ has been studied by employing IR reflectance spectroscopy within the 4…300 K temperature range in the polarized radiation. It has been demonstrated that decreasing the bond distance in the phosphorus chain at low temperatures causes an additional amount of anharmonicity of the corresponding modes, which is manifested in more pronounced temperature dependences of their frequencies and damping coefficients.

1. Introduction

Zinc and cadmium diphosphides ZnP$_2$ and CdP$_2$ belong to promising materials for applications in sensories, optoelectronics and photovoltaics due to their valuable properties portfolio [1, 2]. It is indubitable that successful application of ZnP$_2$ and CdP$_2$ in the devices that are affected by variable external conditions (*e.g.*, temperature [1]) requires understanding the properties of diphosphides within a wide temperature range.

Among the other physical properties, the vibrational ones at different temperatures are important for fundamental understanding anharmonicity in the lattice potential energy of diphosphides ZnP$_2$ and CdP$_2$. Furthermore, the vibrational properties of the diphosphides at different temperatures provide valuable information for understanding the transport properties and electron-phonon interaction, having influence on the electronic devices performances under different conditions. Recently, we have reported on the effect of

low temperatures on behaviour of Raman active phonons in ZnP$_2$ and CdP$_2$ [3]. After analysis of the Raman spectra of two configurations y(xx)y and y(zz)y, we found that low frequency modes which are attributed to (Zn(Cd)-P, Zn(Cd)-Zn(Cd)) vibrations shift very slightly in comparison with the high frequency modes (P-P) upon temperature change. Conformable results were presented in [4] where the impact of pressure on Raman spectra of ZnP$_2$ was studied. Comparing the influence of low temperatures and pressure on the Raman active modes, we have attributed the observed in [3] phenomena to the buckling of the phosphorus chains with decreasing the bond distance in the chains in ZnP$_2$ and CdP$_2$ at low temperatures. However, to obtain the complete picture of the vibrational properties of diphosphides, the temperature impact on the IR active modes should be also studied. Some preliminary data were reported in [5-7], however, the detailed analysis of behaviour inherent to IR active phonons in ZnP$_2$ and CdP$_2$ is still missing. Thus, to fill this gap, we performed the current research.

This paper has a following structure: after presenting the motivation and goal of this work in the *Introduction* section, we describe preparation of the samples and details of measurements in the *Experimental* section. Analysis of the obtained data is presented in the *Results and Discussion*. *Conclusions* summarize the main finding of this paper.

2. Experimental

Single crystals of tetragonal α-ZnP$_2$ and β-CdP$_2$ studied in this paper were grown from the vapour phase. To grow single crystals, polycrystalline ZnP$_2$ and CdP$_2$ obtained from initial elements by two-temperature way were used [7]. Ampoules with polycrystalline ZnP$_2$ and CdP$_2$ were vacuumized down to 10^{-3} Pa, soldered and put into horizontal and vertical resistance furnace. Single crystals were grown in the conic side of the ampoule. It promotes small critical overcooling, which provides a sufficient speed of material transfer from the evaporation zone to the crystallization one. The set of single crystals in the shape of plates with a size of 2×3×1 mm, which were cut from the boules and then polished. The samples were oriented to (001) and (100) crystallographic planes, this orientation of the optical axis *c* in the studied samples enabled us to study the dielectric permittivity dispersion for *E*//*c* and *E*⊥*c*.
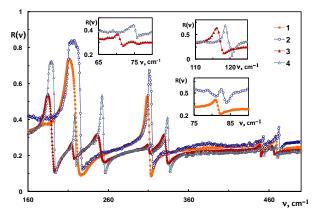
To obtain the reflectance spectra we used Bruker IFS 66 v/s FTIR spectrometer (with a Hg lamp as the radiation source and a He-cooled (4 K) detector) that was equipped with CryoVac cryostat providing variation of the sample temperature within the 4…300 K temperature range. The reflectance spectra were measured within the 60…500 cm^{-1} spectral range in the polarized light for two possible polarizations. The polarizer was a grid of metal strips on a window material that was mounted on a holder and was rotated by step motor. In our experiments, we used a gold mirror (300 nm thick layer of gold deposited on glass plate) with a reflectance of 0.99 in the studied spectral range, as a reference. To normalize the obtained data, the reflectance spectra of the reference and studied samples were measured subsequently. After dividing the sample spectrum by the reference, the final reflectance spectrum was obtained. The angle of radiation incidence was not higher than 10° with respect to the surface normal. The relative measurement error for the reflectance is 2% in the wavelength range from 60 up to 100 cm^{-1} and 0.5% in the wavelength range from 100 up to 500 cm^{-1}.
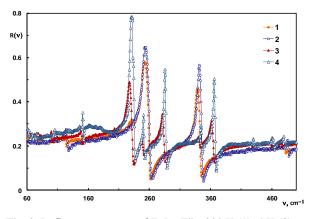
3. Results and discussion

In the unit cell of tetragonal α-ZnP$_2$ and β-CdP$_2$, all atoms are tetrahedrally coordinated and each Metal (Zn or Cd) atom is bonded to 4 Phosphorus atoms, and each Phosphorus atom is bonded to 2 Metal and 2 Phosphorus atoms [8]. The average Metal-Phosphorus distance is 0.24 nm, whereas Phosphorus – Phosphorus distance is approximately 0.21 nm and the ionic radius of

Phosphorus is about 0.1 nm, which enables one to assume that the chemical bond between Phosphorus atoms is rather strong [9]. In structures of diphosphides, Phosphorus atoms form zigzag chains. Continuous bonded chains of phosphorus atoms, which can be regarded as covalently bonded molecules, run through the crystal in the (010) and (100) directions, in the (001) direction all these chains are interrupted by metal atoms. There are four phosphorus chains per unit cell running alternately parallel to (010) or (100) [9]. The Metal atoms are at the center of a deformed tetrahedron and link the Phosphorus chains in 3D structure [8]. The chemical bonding in diphosphides exhibits complex character: Phosphorus–Phosphorus bond carries covalent character, whereas in Metal–Phosphorus bonds a proportion of ionic character (from 16 up to 54% by different estimations) is present [10]. The elementary cell consists of four layers revolved from each other by 90°. The sequence of packing these layers is frequently broken, and instead of four it is possible to observe the multiplets of six, less often five layers [9].

The lattice parameters for ZnP$_2$ crystals of the space symmetry group P4$_1$2$_1$2 are, respectively, $a = b = 0.528$ nm and $c = 1.975$ nm [10]. The lattice parameters of CdP$_2$ crystals of the same space symmetry group exhibits lower values $a = b = 0.508$ nm and $c = 1.859$ nm [11].

According to the group theory [10], vibrational modes in α-ZnP$_2$ and β-CdP$_2$ are distributed among the symmetry types in the following way: $9A_1+9A_2+9B_1+9B_2+18E$. Modes of the symmetry $A_2(z)$ and $E(x, y)$ are IR active, whereas A_1, B_1, B_2, E modes are first-order Raman active. The appearance of the reflectance spectra of the diphosphides ZnP$_2$ and CdP$_2$ that are presented in Figs. 1 and 2, is in good agreement with the data presented in [5-7] regarding the quantity of peaks in each spectrum, their height and width, which confirms the reliability of the obtained data. All the shown peaks exhibit a blue shift upon cooling the sample. At the same time, one can observe an increase in their height, whereas the width of reflectance peaks does not prone any noticeable changes at low temperatures.

Fig. 1. Reflectance spectra of CdP$_2$. *E*//*c*: 300 K (*1*), 4 K (*2*); *E*⊥*c*: 300 K (*3*), 4 K (*4*).

Fig. 2. Reflectance spectra of ZnP_2. $E\|c$: 300 K (1), 4 K (2); $E\perp c$: 300 K (3), 4 K (4).

To fit the experimental spectra of ZnP_2 and CdP_2 in the studied spectral range at temperatures of 4, 50, 100, 150, 200, 250 and 300 K, we used a permittivity model $\varepsilon(v)$ presented as a sum of the phonon contributions, which were modeled by Lorentz oscillators in the following form [12]:

$$\varepsilon(v) = \varepsilon_1(v) + i\varepsilon_2(v) = \varepsilon_\infty + \sum_{j=1}^{N} \frac{S_j v^2}{v_j^2 - v^2 - i\gamma_j v}, \qquad (1)$$

where $\varepsilon_1(v)$ is the real part of the permittivity, while $\varepsilon_2(v)$ is the imaginary part, v_j and γ_j are the frequency and damping coefficients of the *j*-th oscillator, respectively; S_j is the oscillator strength. For the quantitative analysis of the temperature dependent reflectance peaks' behavior, we took a detailed look at the evolution of parameters of Lorentz oscillators. In Fig. 3, we present the typical temperature dependence of the frequency v, damping coefficient γ and strength *S* used to fit some reflectance spectra of ZnP_2 and CdP_2. The parameters of all other phonon peaks exhibit similar temperature
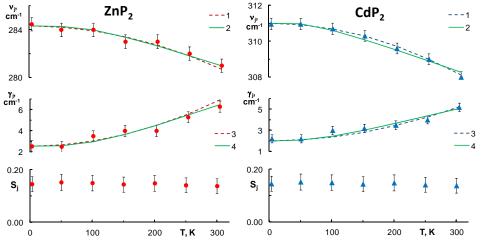
dependences. In Fig. 3, one can notice that the blue shift of the phonon peaks clearly seen in Figs. 1 and 2 results in the increase of the frequency v whereas increase in peaks' amplitude results in the decrease of the damping coefficient γ at lower temperatures. This anharmonical behaviour of infrared active modes resembles that of Raman active modes in ZnP_2 and CdP_2 studied in [3]. The anharmonic frequency shift is the result of the several frequency dependent and independent contributions [13]. In [13] and [14], it was assumed that combination of the optical and acoustical phonons can provide the most important decay channels for the optical phonons. In Fig. 3, we do not observe any trends in the temperature behaviour of the oscillator strength *S*, it remains almost constant within the studied temperature range. This finding can be explained by the fact that the parameter *S* mainly depends on the polarizability of the vibrating unit, which in our case does not change upon cooling down the sample.

Very often anharmonic frequency and damping shifts are characterized by $\Delta v/\Delta T$ and $\Delta\gamma/\Delta T$. However, mode frequencies and dampings need to calculate $\Delta v/\Delta T$ and $\Delta\gamma/\Delta T$, are obtained from the fit of experimental spectra and, therefore, contain an error. In addition, as one see in Fig. 3, both $v(T)$ and $\gamma(T)$ are not linear. On the other hand, the temperature dependence of the observed phonon frequencies and damping coefficients can be satisfactory fitted by a trend line of a parabolic shape in accord with the following relations:

$$v(T) = v_0 - \alpha T^2, \qquad (2)$$

$$\gamma(T) = \gamma_0 + \beta T^2 \qquad (3)$$

with $v_0(\gamma_0)$ being the 0 K limit of the frequency (damping), the parameter $\alpha(\beta)$ which describes the "curvature" of the anharmonic temperature dependence of the mode frequency (damping). The following estimations of the temperature impacts on the frequencies and damping was proposed in [15]:

Fig. 3. Temperature dependence of the oscillators' parameters. *1* – fit by Eq. (2), *2* – fit by Eq. (4), *3* – fit by Eq. (3), *4* – fit by Eq. (5).

Table 1. Temperature dependence of the IR phonon frequency in CdP$_2$ and ZnP$_2$. Fit parameters.

				CdP$_2$							
№	Assignment	ν_{5K}, cm^{-1}	C_j	α, cm^{-1}/K^2	$\Delta\nu/\Delta T$	№	Assignment	ν_{5K}, cm^{-1}	C_j	α, cm^{-1}/K^2	$\Delta\nu/\Delta T$
1	Cd-P, Cd-Cd	83	$2.2 \cdot 10^{-2}$	$2.6 \cdot 10^{-5}$	$6.5 \cdot 10^{-3}$	1	Cd-P, Cd-Cd	72	$2.8 \cdot 10^{-2}$	$1.8 \cdot 10^{-5}$	$4.9 \cdot 10^{-3}$
2		216	$2.8 \cdot 10^{-2}$	$7.0 \cdot 10^{-5}$	$2.0 \cdot 10^{-2}$	2		119	$2.6 \cdot 10^{-2}$	$3.6 \cdot 10^{-5}$	$8.8 \cdot 10^{-3}$
3		311	$9.2 \cdot 10^{-3}$	$2.8 \cdot 10^{-5}$	$1.0 \cdot 10^{-2}$	3		189	$2.3 \cdot 10^{-2}$	$4.6 \cdot 10^{-5}$	$1.3 \cdot 10^{-2}$
4		453	$1.2 \cdot 10^{-2}$	$4.5 \cdot 10^{-5}$	$1.4 \cdot 10^{-2}$	4		218	$2.0 \cdot 10^{-2}$	$5.0 \cdot 10^{-5}$	$1.1 \cdot 10^{-2}$
5	P-P	473	$1.0 \cdot 10^{-2}$	$4.5 \cdot 10^{-5}$	$1.3 \cdot 10^{-2}$	5		252	$2.0 \cdot 10^{-2}$	$8.0 \cdot 10^{-5}$	$2.0 \cdot 10^{-2}$
						6		313	$9.5 \cdot 10^{-3}$	$4.0 \cdot 10^{-5}$	$9.8 \cdot 10^{-3}$
						7		334	$1.2 \cdot 10^{-2}$	$6.0 \cdot 10^{-5}$	$1.3 \cdot 10^{-2}$
						8	P-P	453	$8.0 \cdot 10^{-3}$	$7.0 \cdot 10^{-5}$	$1.6 \cdot 10^{-2}$
						9		469	$8.0 \cdot 10^{-3}$	$8.0 \cdot 10^{-5}$	$1.8 \cdot 10^{-2}$
Average			$1.3 \cdot 10^{-2}$	$3.6 \cdot 10^{-5}$	$1.1 \cdot 10^{-2}$				$2.1 \cdot 10^{-2}$	$5.3 \cdot 10^{-5}$	$1.3 \cdot 10^{-2}$
				ZnP$_2$							
№	Assignment	ν_{5K}, cm^{-1}	C_j	α, cm^{-1}/K^2	$\Delta\nu/\Delta T$	№	Assignment	ν_{5K}, cm^{-1}	C_j	α, cm^{-1}/K^2	$\Delta\nu/\Delta T$
1	Zn-P, Zn-Zn	125	$2.6 \cdot 10^{-2}$	$2.6 \cdot 10^{-5}$	$8.4 \cdot 10^{-3}$	1	Zn-P, Zn-Zn	102	$3.3 \cdot 10^{-2}$	$2.0 \cdot 10^{-5}$	$6.8 \cdot 10^{-3}$
2		251	$1.5 \cdot 10^{-2}$	$3.0 \cdot 10^{-5}$	$8.4 \cdot 10^{-3}$	2		151	$3.0 \cdot 10^{-2}$	$3.0 \cdot 10^{-5}$	$6.8 \cdot 10^{-3}$
3		340	$1.3 \cdot 10^{-2}$	$3.5 \cdot 10^{-5}$	$1.0 \cdot 10^{-2}$	3		229	$2.0 \cdot 10^{-2}$	$3.5 \cdot 10^{-5}$	$1.0 \cdot 10^{-2}$
4	P-P	487	$1.3 \cdot 10^{-2}$	$4.2 \cdot 10^{-5}$	$1.4 \cdot 10^{-2}$	4		251	$1.7 \cdot 10^{-2}$	$3.0 \cdot 10^{-5}$	$8.8 \cdot 10^{-3}$
						5		284	$1.8 \cdot 10^{-2}$	$4.0 \cdot 10^{-5}$	$1.2 \cdot 10^{-2}$
						6		345	$1.9 \cdot 10^{-2}$	$4.5 \cdot 10^{-5}$	$1.4 \cdot 10^{-2}$
						7		366	$1.4 \cdot 10^{-2}$	$4.3 \cdot 10^{-5}$	$1.2 \cdot 10^{-2}$
						8	P-P	432	$1.2 \cdot 10^{-2}$	$4.9 \cdot 10^{-5}$	$1.5 \cdot 10^{-2}$
						9		463	$1.1 \cdot 10^{-2}$	$5.2 \cdot 10^{-5}$	$1.4 \cdot 10^{-2}$
						10		481	$1.1 \cdot 10^{-2}$	$5.5 \cdot 10^{-5}$	$1.5 \cdot 10^{-2}$
Average			$1.1 \cdot 10^{-2}$	$2.2 \cdot 10^{-5}$	$6.7 \cdot 10^{-3}$				$2.3 \cdot 10^{-2}$	$4.4 \cdot 10^{-5}$	$1.3 \cdot 10^{-2}$

Table 2. Temperature dependence of the IR phonon damping in CdP$_2$ and ZnP$_2$. Fit parameters.

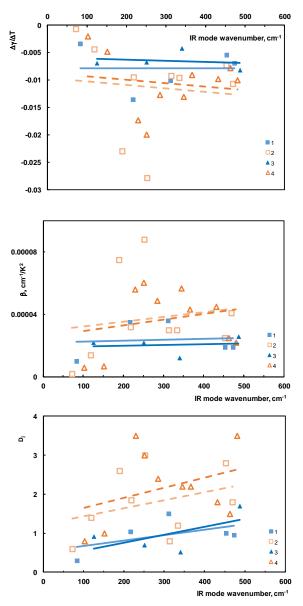| №	Assignment	γ_{5K}, cm^{-1}	D_j	β, cm^{-1}/K^2	$\Delta\gamma/\Delta T$	№	Assignment	γ_{5K}, cm^{-1}	D_j	β, cm^{-1}/K^2	$\Delta\gamma/\Delta T$
				CdP$_2$							
1	Cd-P, Cd-Cd	4.00	0.3	$1.0\cdot10^{-5}$	$-3.4\cdot10^{-3}$	1	Cd-P, Cd-Cd	0.30	0.6	$2.0\cdot10^{-6}$	$-6.8\cdot10^{-4}$
2		3.70	1.0	$3.5\cdot10^{-5}$	$-1.4\cdot10^{-3}$	2		0.80	1.4	$1.4\cdot10^{-5}$	$-4.4\cdot10^{-3}$
3		2.00	1.5	$3.6\cdot10^{-5}$	$-1.0\cdot10^{-3}$	3		2.60	2.6	$7.5\cdot10^{-5}$	$-2.3\cdot10^{-2}$
4		1.20	1.0	$1.9\cdot10^{-5}$	$-5.4\cdot10^{-3}$	4		1.47	1.9	$3.2\cdot10^{-5}$	$-9.5\cdot10^{-3}$
5	P-P	1.85	0.9	$1.9\cdot10^{-5}$	$-6.9\cdot10^{-3}$	5		2.69	3.0	$8.8\cdot10^{-5}$	$-2.8\cdot10^{-2}$
						6		4.00	0.8	$3.0\cdot10^{-5}$	$-9.2\cdot10^{-3}$
						7		2.47	1.2	$3.0\cdot10^{-5}$	$-9.6\cdot10^{-3}$
						8	P-P	0.80	2.8	$2.5\cdot10^{-5}$	$-7.3\cdot10^{-3}$
						9		1.80	1.8	$4.1\cdot10^{-5}$	$-1.1\cdot10^{-2}$
				Average							
			0.8	$2.0\cdot10^{-5}$	$-6.6\cdot10^{-3}$				1.7	$3.7\cdot10^{-5}$	$-1.1\cdot10^{-2}$
				ZnP$_2$							
1	Zn-P, Zn-Zn	3.65	0.9	$2.2\cdot10^{-5}$	$-6.9\cdot10^{-3}$	1	Zn-P, Zn-Zn	2.40	0.8	$6.0\cdot10^{-6}$	$-2.0\cdot10^{-3}$
2		4.73	0.7	$2.2\cdot10^{-5}$	$-6.7\cdot10^{-3}$	2		2.00	1.0	$6.9\cdot10^{-6}$	$-4.8\cdot10^{-3}$
3		3.39	0.5	$1.2\cdot10^{-5}$	$-4.2\cdot10^{-3}$	3		1.80	3.5	$5.6\cdot10^{-5}$	$-1.7\cdot10^{-2}$
4	P-P	1.80	1.7	$2.6\cdot10^{-5}$	$-8.2\cdot10^{-3}$	4		2.60	3.0	$6.0\cdot10^{-5}$	$-2.0\cdot10^{-2}$
						5		2.53	2.4	$4.9\cdot10^{-5}$	$-1.3\cdot10^{-2}$
						6		2.74	2.2	$5.7\cdot10^{-5}$	$-1.3\cdot10^{-2}$
						7		1.87	2.2	$4.3\cdot10^{-5}$	$-9.0\cdot10^{-3}$
						8	P-P	1.59	1.8	$4.5\cdot10^{-5}$	$-9.8\cdot10^{-3}$
						9		4.08	1.5	$2.5\cdot10^{-5}$	$-7.8\cdot10^{-3}$
						10		0.57	3.5	$2.2\cdot10^{-5}$	$-1.0\cdot10^{-2}$
				Average							
			0.6	$1.4\cdot10^{-5}$	$-4.3\cdot10^{-3}$				2.2	$4.1\cdot10^{-5}$	$-1.2\cdot10^{-2}$

Fig. 4. Fit parameters that describe temperature behaviour of the phonon frequency versus the corresponding phonon frequency. CdP$_2$: **E**//c (*1*), **E**⊥c (*2*); ZnP$_2$: **E**//c (*3*), **E**⊥c (*4*).

Fig. 5. Fit parameters that describe temperature behaviour of the phonon damping versus the corresponding phonon frequency. CdP$_2$: **E**//c (*1*), **E**⊥c (*2*); ZnP$_2$: **E**//c (*3*), **E**⊥c (*4*).

$$\nu = \nu_0 \left(1 - \frac{C_j}{\exp(\Theta/T) - 1} \right), \qquad (4)$$

$$\gamma = \gamma_0 \left(1 + \frac{D_j}{\exp(\Theta/T) - 1} \right), \qquad (5)$$

where $\nu_0(\gamma_0)$ is the frequency (damping) at 0 K, T – temperature, C_j and D_j are the fitting parameters determining the strength of the anharmonic contributions, Θ is the Debye temperature (206 K for CdP$_2$ and 280 K for ZnP$_2$ [16]). As one see in Fig. 3, Eqs. (2) to (5) can be satisfactory applied to fit the temperature dependences of the phonon frequency and damping.

After obtaining the parameters that describe the anharmonicity of the phonon modes in ZnP$_2$ and CdP$_2$ (Tables 1 and 2), it is interesting to study their distribution on phonon frequencies for both **E**//c and **E**⊥c. In [4, 10], the low frequency Raman peaks were attributed to the Zn-P and Zn-Zn modes, whereas the high frequency peaks were assigned to the internal vibrations of the phosphorus chain. Due to the similar structure, this assignment should also be correct for the case of CdP$_2$. In Figs. 4 and 5, we have plotted the parameters from Tables 1 and 2 vs. corresponding phonon frequencies, for the better visualization these dependences were supplemented with linear trend lines. As seen from Figs. 4 and 5, low frequency phonons are either practically temperature

independent or exhibit very slight softening, whereas higher frequency modes are more sensitive and show stronger temperature dependence. It is remarkable, that on the one hand, the slope of the trend lines in Figs. 4 and 5 of ZnP_2 and CdP_2 is almost the same within the sample orientation $E\|c$ or $E\perp c$, as expected due to the similarity in the structure of ZnP_2 and CdP_2. On the other hand, the slope of the trend lines depends on orientation of the sample: for $E\perp c$ exhibit significantly stronger temperature dependence of the fit parameters from Eqs. (2) to (5). According to [10], the chains formed by phosphorus atoms are oriented in parallel alternately to (010) or (100), *i.e.*, lie along the perpendicular to the *c*-axis. This means that in both orientations $E\|c$ or $E\perp c$ the lower frequency Zn(Cd)-P and Zn(Cd)-Zn(Cd) modes exhibit very slight softening, whereas the frequency and damping coefficients of internal vibrations of the phosphorus chains possessing additional amount of anharmonicity, which is manifested in their stronger temperature dependence. This finding is supported by the Grueneisen anharmonical parameters of CdP_2 and ZnP_2 along and perpendicular to the *c*-axis, which were reported in [16]. The latter is in the agreement with the previously reported results [3], where the similar phenomena were attributed mainly to the buckling of the phosphorus chain with decreasing the bond distance in the chain at low temperatures.

4. Conclusions

By applying the temperature dependent reflectance spectroscopy to CdP_2 and ZnP_2 single crystals in the range of IR active phonons, we found that modes corresponding to the vibrations of the phosphorus chains are more temperature dependent, *i.e.*, exhibit an additional amount of the anharmonicity, which can be mainly explained by decreasing the bond distance in the chain at low temperatures. The obtained results might be useful for studying the modes anharmonicity impact on dispersion of surface polaritons in the diphosphides CdP_2 and ZnP_2.

References

1. S.F. Marenkin, V.M. Trukhan, *Phosphides and Arsenides of Zn and Cd*. Minsk: IP A.N. Varaksin, 2010 (in Russian).
2. D. Stepanchikov and S. Shutov, Cadmium phosphide as a new material for infrared converters // *Semiconductor Physics, Quantum Electronics and Optoelectronics*, **9**, no. 4, p. 40-44 (2006).
3. K.V. Shportko, R. Rueckamp, T.V. Shoukavaya, V.M. Trukhan, H.M. El-Nasser, and E.F. Venger, Effect of the low temperatures on the Raman active vibrational modes in ZnP_2 and CdP_2 // *Vib. Spectrosc.* **87**, p. 173-181 (2016).
4. T. Jayaraman, A. Maines, R.G. Chattopadhyay, Effect of high pressure on the vibrational modes and the energy gap of ZnP_2 // *Pramanan – J. Phys.* **27**, no. 1–2, p. 291-297 (1986).
5. K.V. Shportko, Yu.A. Pasechnik, M. Wuttig, R. Rueckamp, V.M. Trukhan, T.V. Haliakevich // Plasmon–phonon contribution in the permittivity of ZnP_2 single crystals in FIR at low temperatures // *Vib. Spectrosc.* **50**, p. 209-213 (2009).
6. K.V. Shportko, R. Rückamp, V.M. Trukhan, and T.V. Shoukavaya, Reststrahlen of CdP_2 single crystals at low temperatures // *Vib. Spectrosc.* **73**, p. 111-115 (2014).
7. K.V. Shportko, A.D. Izotov, V.M. Trukhan, T.V. Shelkovaya, and E.F. Venger, Effect of temperature on the region of residual rays of CdP_2 and ZnP_2 single crystals // *Russ. J. Inorg. Chem.* **59**, no. 9, p. 986-991 (2014).
8. C. Manolikas, J. van Tendeloo, and S. Amelinckx, The 'devil's staircase' in CdP_2 and ZnP_2 // *phys. status solidi*, **97**, no. 1, p. 87-102 (1986).
9. J.G. White, The crystal structure of the tetragonal modification of ZnP_2 // *Acta Crystallogr.* **18**, no. 2, p. 217-220 (1965).
10. I.I. Gorban, I.S. Gorinya, V.A. Dashkovskaya, R.A. Lugovoi, V.I. Makovetskaya, A.P. Tychina // One and two-phonon states in tetragonal ZnP_2 and CdP_2 crystals // *Phys. Status Solidi* (*b*), 86, p. 419-424 (1978).
11. K.B. Aleinikova, A.I. Kozlov, S.G. Kozlova, and V.V. Sobolev, Electronic and crystal structures of isomorphic ZnP_2 and CdP_2 // *Phys. Solid State*, **44**, no. 7, p. 1257-1262 (2002).
12. M. Fox, *Optical Properties of Solids*. Oxford University Press, 2006.
13. B. Hart, T.R. Aggarwai, R.I. Lax, Temperature dependence of Raman scattering in silicon // *Phys. Rev. B*, **1**, no. 2, p. 638-642 (1970).
14. J. Menéndez and M. Cardona, Temperature dependence of the first-order Raman scattering by phonons in Si, Ge, and a-Sn: Anharmonic effects // *Phys. Rev. B*, **29**, no. 4, p. 2051-2059 (1984).
15. T. Rudolf, C. Kant, F. Mayr, J. Hemberger, V. Tsurkan, and A. Loidl, Polar phonons and spin-phonon coupling in $HgCr_2S_4$ and $CdCr_2S_4$ studied with far-infrared spectroscopy // *Phys. Rev. B*, **76**, p. 174307 (2007).
16. H.L. Soshnikov, L.E. Trukhan, V.M. Haliakevich, T.V. Soshnikava, Dielectric and elastic properties of CdP_2, ZnP_2 and $ZnAs_2$ single crystals // *Mold. J. Phys. Sci.* **4**, no. 2, p. 201-210 (2005).